Science Arts & Métiers (SAM)

is an open access repository that collects the work of Arts et Métiers Institute of Technology researchers and makes it freely available over the web where possible.

This is an author-deposited version published in: https://sam.ensam.eu
Handle ID: .http://hdl.handle.net/10985/23605

To cite this version :

Jinyang XU, Mohamed EL MANSORI, Julien VOISIN, Ming CHEN, Fei REN - On the interpretation of drilling CFRP/Ti6Al4V stacks using the orthogonal cutting method: Chip removal mode and subsurface damage formation - Journal of Manufacturing Processes - Vol. 44, p.435-447 - 2019

Any correspondence concerning this service should be sent to the repository Administrator : scienceouverte@ensam.eu

Arts et Métiers Institute of Technology

On the interpretation of drilling CFRP/Ti6Al4V stacks using the orthogonal cutting method: Chip removal mode and subsurface damage formation

Jinyang Xu[a,*], Mohamed El Mansori[b,c], Julien Voisin[b], Ming Chen[a], Fei Ren[d]

[a] State Key Laboratory of Mechanical System and Vibration, School of Mechanical Engineering, Shanghai Jiao Tong University, Shanghai 200240, China
[b] MSMP – EA 7350, Arts et Métiers ParisTech, Rue Saint Dominique, BP 508, Châlons-en-Champagne 51006, France
[c] Department of Mechanical Engineering, Texas A&M University, College Station, TX 77840, USA
[d] Shanghai Aerospace Equipments Manufacturer Co., Ltd., Shanghai 200245, China

ARTICLE INFO

Keywords:
CFRP composites
Titanium alloys
Orthogonal cutting
Drilling processes
Cutting mechanisms
Hole quality

ABSTRACT

The present paper aims to utilize the orthogonal cutting method to offer an enhanced interpretation of the drilling process on CFRP/Ti6Al4V stacks. It contributes to relating the chip separation modes of the orthogonal cutting of multilayer CFRP/Ti6Al4V stacks with their drilling characteristics. A particular focus was made to identify the effect of different cutting sequence strategies on the 3D topographies and defects formation of cut CFRP/Ti6Al4V stacks as well as the mechanisms controlling the drilling of the stack interface. Three configurations of orthogonal cutting operations considering both the impact of varying cutting sequence strategies and the combined interface machining were implemented and the *in-situ* chip removal characteristics were documented. Mechanical drilling of CFRP/Ti6Al4V stacks was performed subjected to varying cutting sequences and process parameters. Aspects involving the cutting forces, drilling-induced damage as well as the machined hole morphologies were carefully addressed with respect to the used cutting conditions. The obtained orthogonal cutting results were utilized to facilitate the stack drilling comprehension. The results discussed in this paper highlight the vital role of the cutting sequence strategy in the stack machinability and permit an enhanced interpretation of drilling this multilayer material.

1. Introduction

In the modern aerospace industry, there is an ongoing demand for the use of lightweight materials, motivated by the ecological requirements for minimized fuel consumption as well as for economic reasons including low operating costs, long maintenance cycle, and reduction of life-cycle-cost [1]. In such a circumstance, compound stacks uniting fibrous composites and lightweight metals emerge and serve as a promising alternative to conventional standard composites and metal alloys in a variety of aerospace applications due to their enhanced mechanical properties and improved structural functions [2,3]. Materials made of multilayers of carbon fiber reinforced polymers and titanium alloys are a typical example of a metallic-composite stack, being widely used for the skin segments, fuselages, and wing segments of an aircraft [2,4]. To assemble the multilayer materials by bolt joints or rivet connections, mechanical drilling becomes a necessity. However, these hybrid composite stacks are rather difficult to drill, which often leads to poor hole quality, severe tool wear and short tool lifetime as both workpiece materials show completely different machinability characteristics.

Drilling CFRP/Ti6Al4V stacks involves a combination of powdery and serrated chip formation due to the predominance of chip separation modes of brittle fracture and elastoplastic deformation. The dissimilar machining behaviors of fibrous composites and titanium alloys often result in serious physical damage and geometrical imperfections of a cut stack hole, greatly affecting the assembly performance and the fatigue life of the stack-made components. To improve the machinability and surface quality of these hybrid composite stacks, a better understanding of the drilling mechanisms plays a vital role in optimizations of cutting parameters and tool geometries. In recent years, only few endeavors have been devoted to the studies of drilling composite/metal stacks in the open literature. Ramulu et al. [5] conducted an experimental study on the drilling of Gr/Bi-Ti stacks using three kinds of drill materials including HSS, HSS-Co and carbide. Results indicated that the most significant issue arising in the stack drilling was the high cutting temperatures produced by the titanium alloys that increased the interface damage region, burr heights, heat-induced delamination as well as the tool wear. The carbide drills were found to outperform all other tools in

* Corresponding author.
E-mail address: xujinyang@sjtu.edu.cn (J. Xu).

https://doi.org/10.1016/j.jmapro.2019.05.052

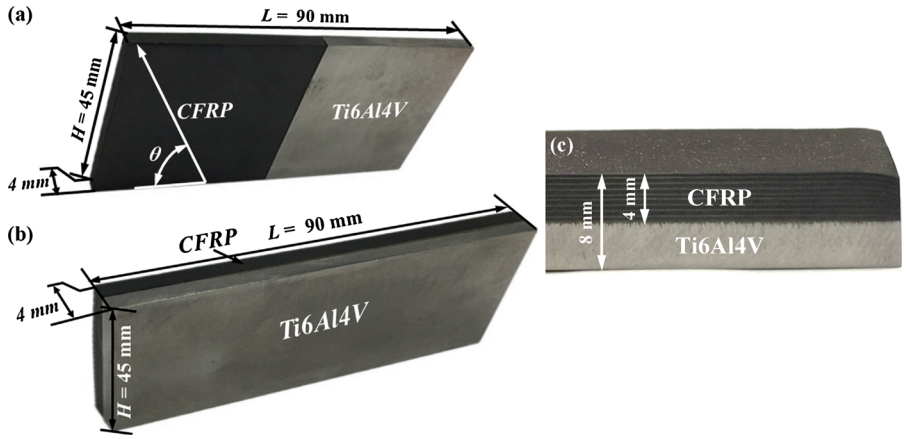

Fig. 1. Photographs showing the CFRP/Ti6Al4V stack workpieces for the (a) orthogonal cutting, (b) interface machining and (c) hole drilling.

terms of longer tool life and minimal surface damage. Brinksmeier et al. [1] performed the orbital drilling and conventional drilling of Al/CFRP/Ti stacks. It was found that the orbital drilling led to lower process temperatures and lower feed forces in all stacked material layers while in the conventional drilling the local temperature peaks due to high cutting speeds or effluent titanium chips damaged the surface layer of the CFRP material. Isbilir and Ghassemieh [6] evaluated the tool life and hole quality in drilling CFRP/Ti6Al4V stacks and their individual layers under different cutting conditions. The results showed that the delamination increased with the feed rate but decreased with the cutting speed. Drilling CFRP in a stack form could lead to much smaller delamination damage due to the backup effects of the titanium phase. The tool life was significantly shortened in the drilling of stacks because of the combined wear of each stacked phase. Park et al. [7] found that abrasion caused by the carbon fibers as well as the titanium adhesion was the key tool wear patterns during drilling of CFRP/Ti6Al4V stacks. Prabukarthi et al. [8] evaluated the performance of different modified twist drills in drilling CFRP/Ti6Al4V stacks using the acoustic emission technique. The authors found that both the helix and point angles were the key factors affecting the tool performance, and drills with a high helix angle and a low point angle could produce the lowest thrust forces while drilling the composite/metal stacks. Moreover, some other scholars sought to identify the feasibility of non-traditional drilling techniques for CFRP/Ti6Al4V stacks. Cong et al. [9] and Sanda et al. [10] applied the technique of ultrasonic vibration assisted (UVA) drilling for CFRP/Ti6Al4V stacks and found that the use of UVA drilling could greatly improve the machinability of the examined hybrid composite stack *i.e.*, decreasing the drilling forces, cutting temperatures, surface roughness as well as the hole damage compared with the conventional twist drilling. Recently, Impero et al. [3] compared the performance of wet and cryogenic drilling of CFRP/Ti6Al4V stacks and results indicated that the cryogenic machining was more feasible for the drilling of CFRP/Ti6Al4V stacks in terms of lower thrust force and torque. Apart from the drilling investigations of CFRP/Ti6Al4V stacks, Xu and El Mansori [11,12] conducted several research works concerning the orthogonal cutting of the composite/metal stacks by addressing a variety of machining aspects. However, a detailed study correlating the drilling mechanisms of the multilayer stack and the simplified orthogonal cutting is significantly lacking. The present work is thus aimed at utilizing the orthogonal cutting method to offer an enhanced interpretation of the drilling process on the CFRP/Ti6Al4V stacks. It contributes to relating the chip separation modes of the orthogonal cutting of multilayer CFRP/Ti6Al4V stacks with their drilling characteristics. A particular focus was made to identify the effect of different cutting sequence strategies on the 3D topographies and defects formation of cut CFRP/Ti6Al4V stacks, which was not investigated in our previous studies. Additionally, this paper addresses not only the impact of different cutting sequence strategies on the stack machinability but also the combined interface machining *i.e.* cutting the two stacked constituents simultaneously to model and interpret the drilling of the stack interface, which was not treated in the scientific literature. The stack drilling process was abstracted into three configurations of orthogonal cutting considering both the impacts of two cutting sequences and the stack interface machining. The orthogonal cutting operations were conducted on the UD-CFRP/Ti6Al4V stacks with varying fiber orientation in order to identify the fundamental machining mechanisms. The *in-situ* chip removal process under the orthogonal cutting was documented using a high-speed charge coupled device (CCD) camera to facilitate the stack machinability comprehension. Afterward, the drilling tests of these multilayer stacks were carried out. The corresponding drilling forces, surface damage and morphologies were investigated. The orthogonal cutting findings were correlated with the drilling responses of CFRP/Ti6Al4V stacks, allowing for an enhanced interpretation of the stack machinability.

2. Experimental details

2.1. Workpieces and cutting tools

The experiments performed in this work consist of the orthogonal cutting subjected to different cutting sequences, the stack interface machining and the hole drilling. Two difficult-to-cut materials representative of aircraft components were utilized including T300/914 carbon/epoxy composites and Ti6Al4V alloys. To address the mechanisms and strategies for the composite/titanium stack drilling in one shot, the process can be represented, in the simplest terms, as force traveling on the surface of the stack workpiece. In the current work, the orthogonal cutting derived from the multilayer stack drilling was adopted and the experiments were conducted on the composite/metal stacks constituted by unidirectional T300/914 laminates and Ti6Al4V sheets that possess the identical dimensions as detailed in Fig. 1. Regarding the hole drilling, the stack specimens constituted by multidirectional T300/914 laminates of $[45^{\circ}/\text{-}45^{\circ}/0^{\circ}/90^{\circ}]_s$ ply orientation and Ti6Al4V alloys were adopted. The CFRP/Ti6Al4V specimen has the total size of 254 mm (length) × 34.5 mm (width) × 8 mm (thickness). The overall morphologies of the utilized workpieces are shown in Fig. 1. To finalize the orthogonal cutting and the stack interface machining, the polycrystalline diamond (PCD) tipped inserts and the MTCVD (Medium Temperature Chemical Vapor Deposition) coated inserts consisting of multilayer ($TiN + Al_2O_3 + TiCN$) coatings were respectively utilized. Note that each insert has the identical geometries of a 0° rake angle and a 7° clearance angle.

The drilling tests were completed using the TiAlN-coated carbide twist drills having a diameter of 6.35 mm provided by Sandvik

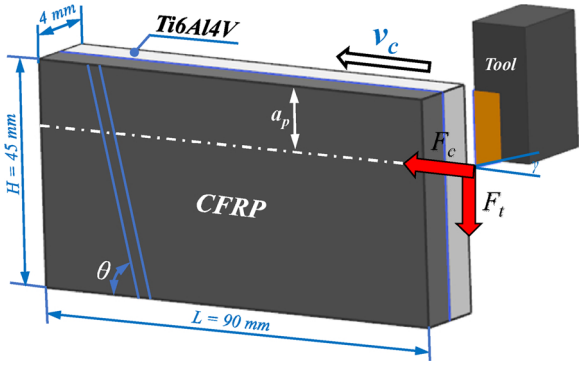

Fig. 2. A schematic diagram illustrating the definitions of the used cutting variables in the CFRP/Ti6Al4V interface machining.

Coromant. The drill has two flutes, a 0.22 mm-length chisel edge, a 27.2° helix angle and a 140° point angle. The utilized TiAlN coating typically deposited by 2–5 μm thick films with hardness ranging between 3000 HV and 3300 HV, is thermally stable up to 900 °C and has a coefficient of friction against steel counterparts between 0.35 and 0.40 [13,14], which can offer high-temperature oxidation resistance and an excellent ability to maintain high hardness at elevated temperatures during the drilling of CFRP/Ti6Al4V stacks.

2.2. Experimental setup and post-process analysis

The orthogonal cutting and interface machining experiments were carried out on a GSP-EL136 shaper under the fixed conditions of 50 m/min cutting speed (v_c) and 0.20 mm depth of cut (a_p). A scheme of the definition of the used cutting variables for the stack interface machining is given in Fig. 2. During machining the CFRP/Ti6Al4V stack was rigidly clamped with 3–5 mm of the specimen exposed between two hard steel plates inside a fixture mounted on a piezoelectric Kistler dynamometer (type 9255B). The Kistler dynamometer was firmly fixed on the shaper table connected with a multichannel charge amplifier and a PC in order to acquire the force signals (cutting force (F_c) and thrust force (F_t)) generated in the chip removal process. The *in-situ* chip formation process was documented by a high-speed CCD camera equipped with a strobed copper-vapor laser illumination system at an acquisition rate of 20,000 fps.

The drilling trials were conducted on a five-axis CNC machining center DMU60 monoBLOCK under the dry cutting conditions. Thrust force and torque generated during drilling of CFRP/Ti6Al4V stacks were measured by a piezoelectric dynamometer (Kistler 9271A). Two different cutting sequences *i.e.* drilling from CFRP to Ti6Al4V and from Ti6Al4V to CFRP were implemented. Since both constituents exhibit disparate machinability behaviors, a compromise selection in drilling parameters was conducted to finalize the one-shot drilling of the metallic-composite stack. In each drilling sequence, a number of new drills were used and the following cutting conditions including a fixed cutting speed (v_c) of 30 m/min and the varying feed rate (f) of 0.03, 0.06, 0.09, 0.12, 0.15 mm/rev were adopted. To get reliable results, each test was repeated three times under the identical cutting conditions.

After the completion of the machining tests, post-process analyses were performed on the resected chips and the machined stack surfaces. The microstructure of titanium chips was characterized using a Nikon toolmaker's microscope after they were mounted in a cold resin. The delamination damage and burr defects of drilled stack holes were quantified using the Nikon toolmaker's microscope. To examine the inner hole wall morphologies, the stack plate was cut into several parts through the hole center using the water-jet machining technique. To minimize the secondary cutting-induced damage on the stack surfaces, resin spraying was made on each drilled hole. The water-jet cutting was performed on a Resato ACM 3015 machine tool at a constant cutting speed of 7 mm/min and a water pressure of 3600 bars. Fig. 3 shows the *in-situ* water-jet machining of one CFRP/Ti6Al4V specimen and the corresponding separated hole parts. The surface topographies and the damage modes of the drilled holes subjected to different cutting sequences were inspected using a white-light interferometer (type Wyko 3300 N T) and a JEOL scanning electron microscope (SEM) (type JSM-5510LV). The obtained results were carefully analyzed and correlated with the used process parameters and cutting sequence strategies.

3. Results and discussion

3.1. Orthogonal cutting characteristics

In machining processes, chip formation characteristics are of great importance for the understanding of the cutting responses of a work material. Fig. 4 shows the typical frames gained by the CCD camera for 0°, 45°, and 90° UD-CFRP/Ti6Al4V stacks operating under the CFRP → Ti sequence. The corresponding force signatures (cutting force (F_c) and thrust force (F_t)) are depicted in Fig. 5. When machining the CFRP composite, discontinuous chips are produced flowing ahead of the tool rake face for all the used fiber orientations. In machining the 0 °CFRP phase of a multilayer stack the mode I fracture initiates along the fiber/matrix interface causing a layer to peel up and to slide on the rake face [15]. Cracks are introduced and propagate along the fiber direction, leading to the debonding of the fiber/matrix interface. The separation of the carbon/epoxy composite is eventually completed through a series of fractures occurring perpendicular to the fiber axis (fracture mode II) due to the combined effects of microbuckling and cantilever bending. The composite chips are basically resected in the form of powdery dust. The machined surface for the 0° UD-CFRP is characterized by fractured fiber surface and smeared matrix being an unequivocal evidence of failure of the fiber/matrix interface as depicted in Fig. 5(b). The surface

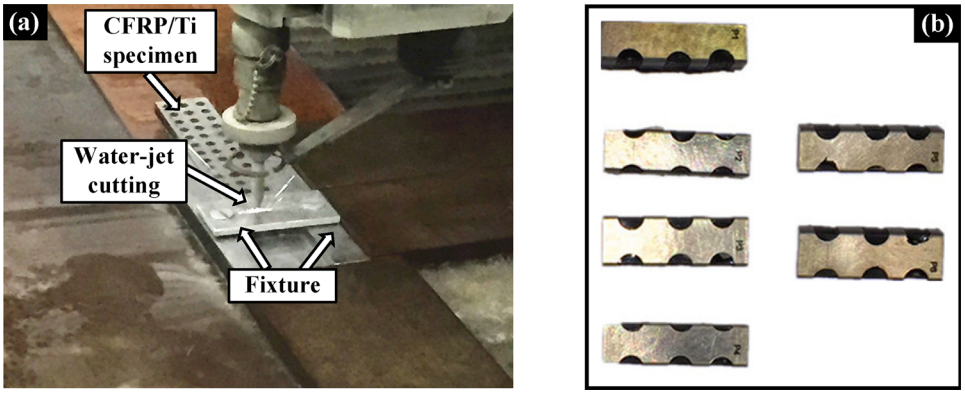

Fig. 3. (a) *In-situ* water-jet machining of one CFRP/Ti6Al4V specimen and (b) several separated hole parts.

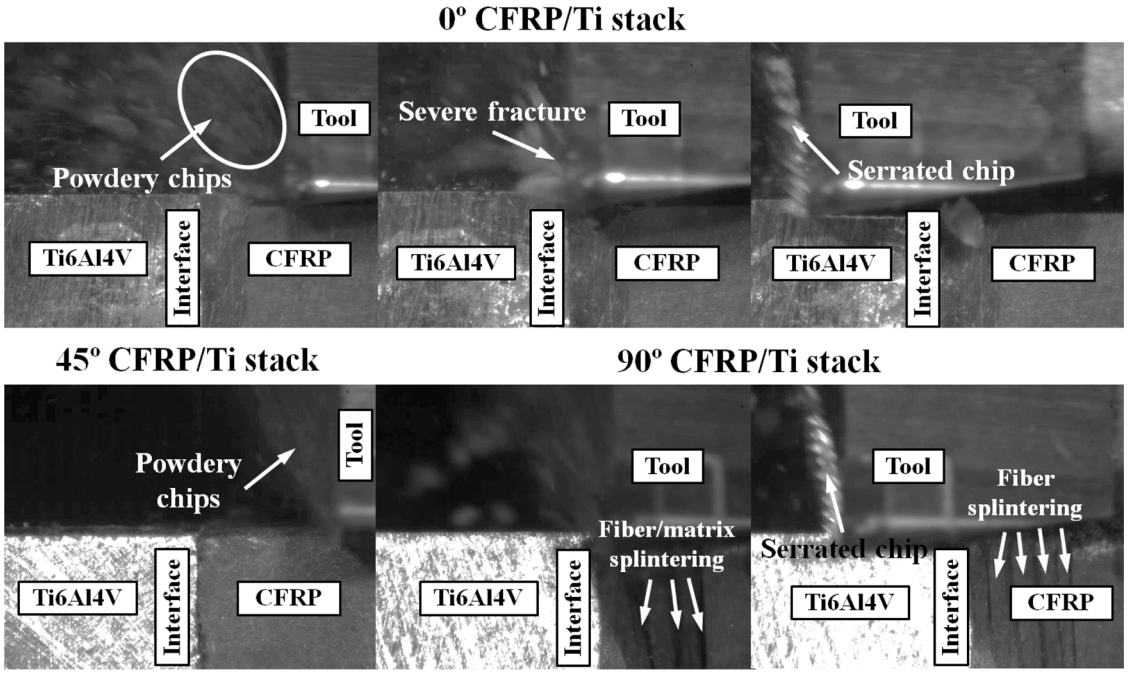

Fig. 4. *In-situ* chip separation process of CFRP/Ti6Al4V orthogonal cutting under the CFRP → Ti sequence (v_c = 50 m/min and a_p = 0.20 mm). (Some images were extracted from [12]).

quality of the present fiber orientation was found as the best in our previous studies [11,12]. As the tool edge fully engages in the chip separation process both the cutting and thrust force signals attain the comparable magnitudes as evidenced in Fig. 5(a). When the tool cuts across the interface region, a sudden increase of the cutting force is identified, which suggests a rapid transition of the chip separation mode. This phenomenon is likely to induce severe cutting vibration and tool chatter that may increase the risk of catastrophic failure of the PCD

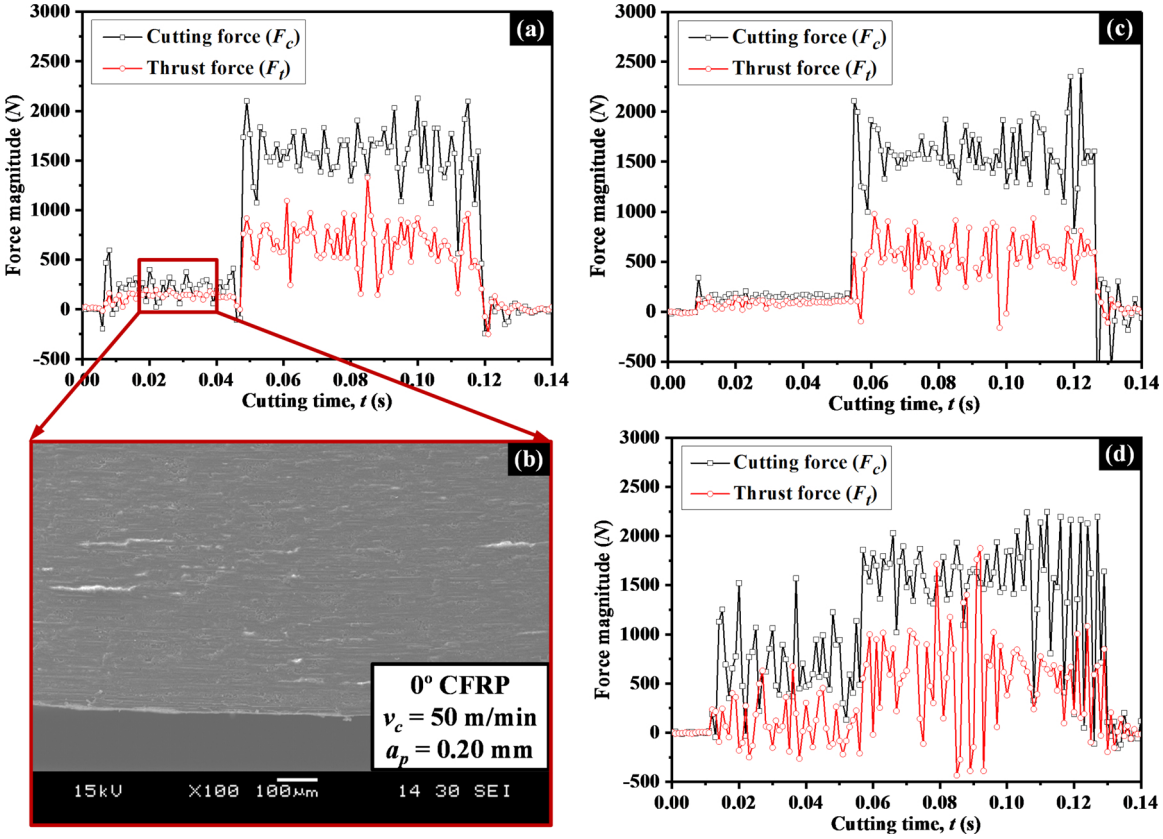

Fig. 5. Evolution of the force profiles in the orthogonal cutting of CFRP/Ti6Al4V stacks under the CFRP → Ti sequence (v_c = 50 m/min and a_p = 0.20 mm): (a) θ = 0°, (b) SEM image of the cut 0 °CFRP surface, (c) θ = 45° and (d) θ = 90°.

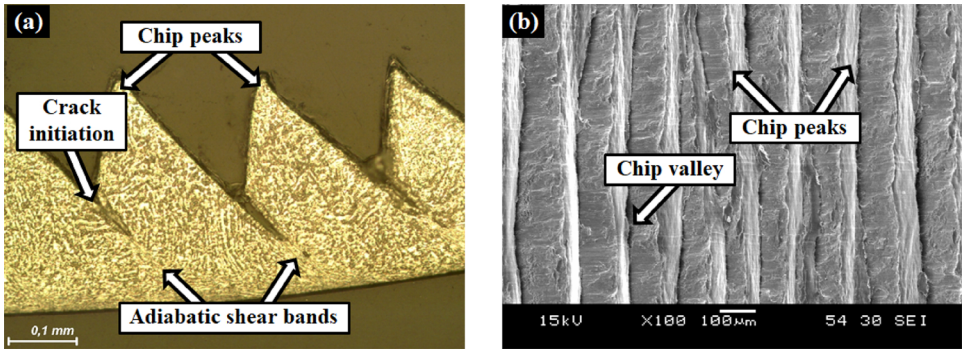

Fig. 6. Microstructures of (a) the cross-section and (b) the free surface of a titanium chip gained in the orthogonal cutting of CFRP/Ti6Al4V stacks.

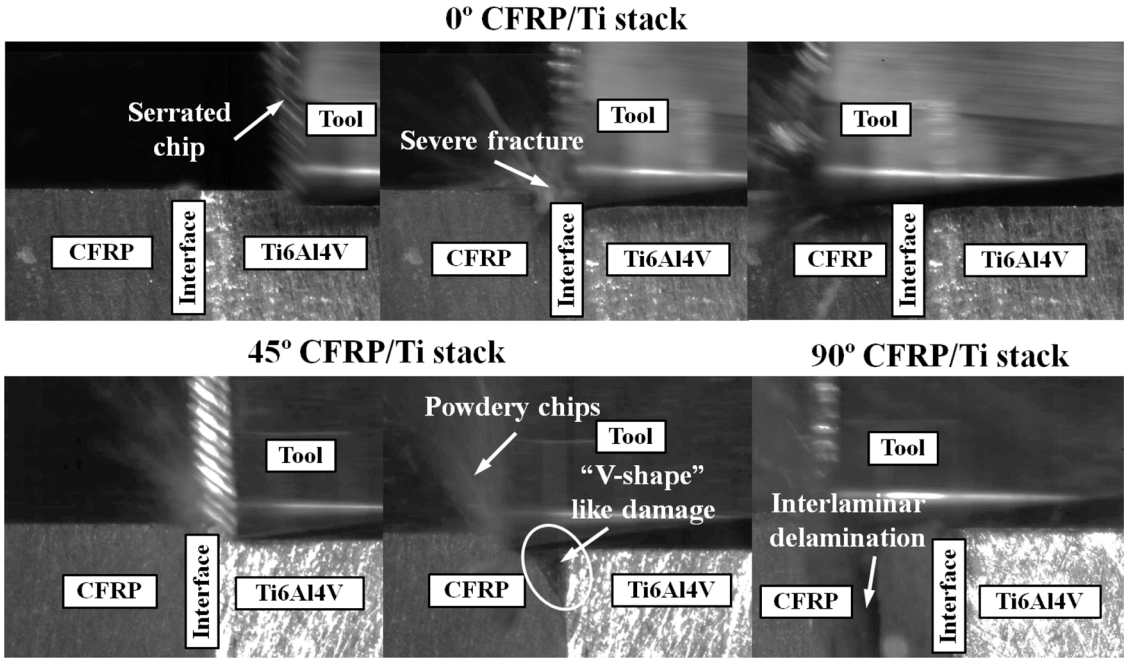

Fig. 7. *In-situ* chip separation process of CFRP/Ti6Al4V orthogonal cutting under the Ti → CFRP sequence (v_c = 50 m/min and a_p = 0.20 mm). (Some images were extracted from [12]).

inserts like micro chipping or edge fracture. As the tool edge attacks the titanium alloy, continuous and serrated chips are generated as a result of the elastoplastic deformation. The titanium chips gained in the stack machining are featured by moderately formed chip segments separated by very narrow bands of highly sheared materials which are known as adiabatic shear bands as depicted in Fig. 6. Such a phenomenon is due to the combination of thermoplastic instability resulting from the adiabatic shearing and the initiation/propagation of cracks inside the primary shear zone (Ref. Fig. 6(a)), which leads to the cyclic force variations as evidenced in Fig. 5(a). When machining a positive fiber orientation configured CFRP/Ti6Al4V stack (*e.g.* θ = 45°), the chip removal mode of the composite phase consists of the compression-induced shear perpendicular to the fiber axis and the interfacial shearing along the fiber direction. The fracture mode II initially occurs under a compressive shear, leading to cracks in fibers above and below the cutting plane. Then, an interfacial shear starts at the vicinity of the primary fracture and propagates in a direction congruent with the fiber orientation until completely releasing the chip. The produced cracks residing within the machined surface can be easily observed by the optical microscope and the material removal mode of the positive fiber orientation is governed by the in-plane shear properties. In the case of cutting a 90 °CFRP/Ti6Al4V stack, serious fiber/matrix splintering and interlaminar delamination are clearly visible via the *in-situ* camera images of Fig. 4. The phenomena are attributed to the severe out-of-plane shear fracture occurring along the fiber/matrix interface with interlaminar deformation induced by the compressive tool load. This can be reflected by the high-frequency fluctuations of the cutting and thrust force signals presented in Fig. 5(d). Owing to the predominance of out-of-plane displacement and interlaminar fracture, the produced cutting and thrust forces appear much higher than those of the 0° and 45 °CFRP phases and seem nearly comparable to those of the titanium phase. Additionally, thanks to the rigid support provided by the adjacent titanium alloy the interface linking both the composite and metallic phases is protected from the interlayer cracking.

Fig. 7 shows the recorded chip separation process of the CFRP/Ti6Al4V stacks under the Ti → CFRP sequence. It is clear that the cutting phenomena observed in the present sequence differ in several aspects from those observed in the CFRP → Ti sequence. When machining the titanium alloy first, the resected titanium chip tends to adhere onto the tool rake face that replaces the tool edge for further separation of the interface and the CFRP phase. The sharp-edged metallic chips could cause severe plowing and scratching to the stack interface resulting in the interlayer fracture regardless of the used fiber orientation. As depicted in the cutting case of 45 °CFRP/Ti6Al4V stacks in Fig. 7, the "V-shape" like notch damage is produced after the tool edge cuts across the interface region. During the cutting of 90 °CFRP/

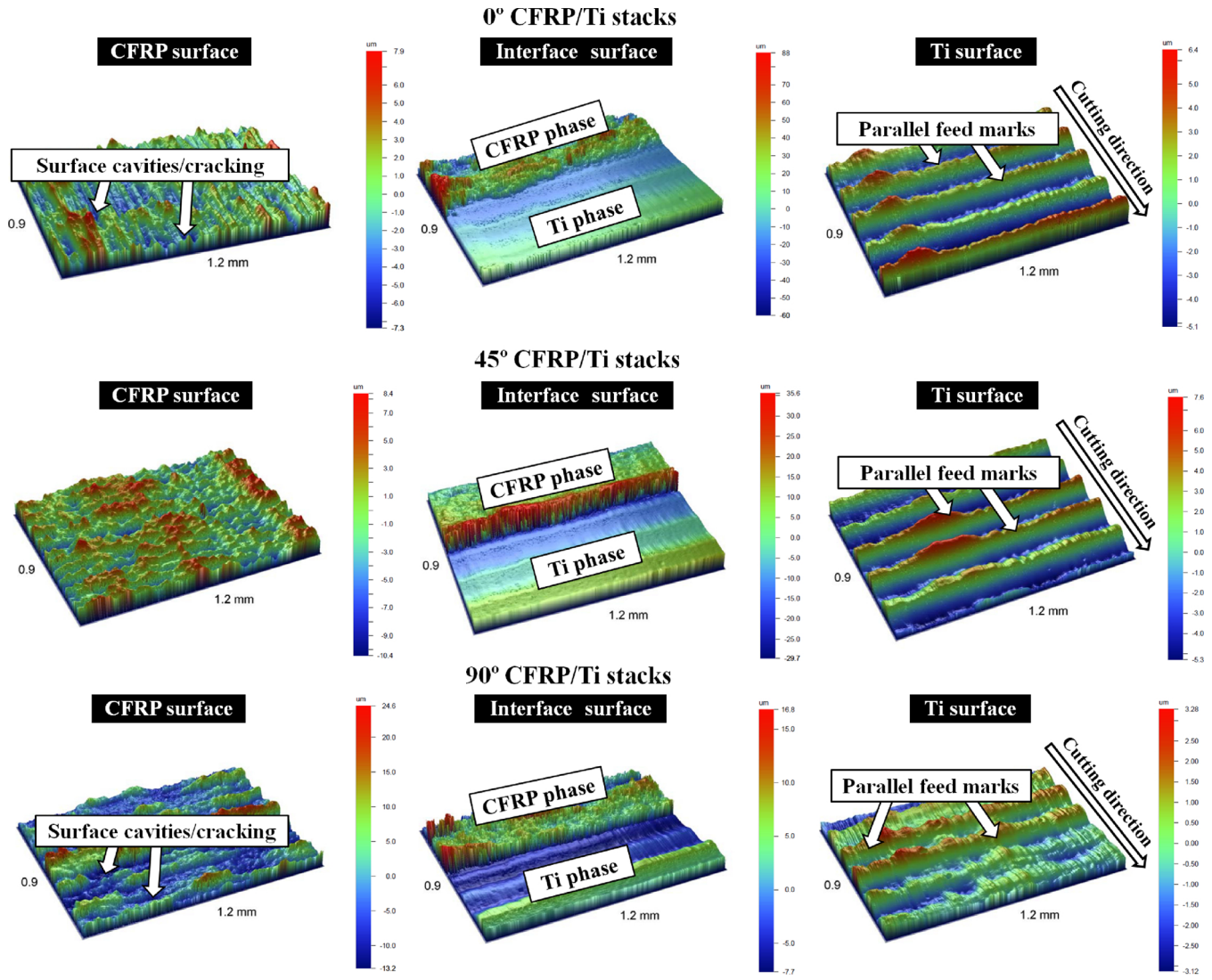

Fig. 8. 3D topographies of the machined stack surfaces under the CFRP → Ti sequence (v_c = 50 m/min and a_p = 0.20 mm).

Ti6Al4V stacks under the Ti → CFRP sequence, the Ti chip adhesion on the tool rake face is observed to plow and rub against the uncut composite layer, leading to a large extent of interlaminar delamination or cracking far beyond the cut surface. The above analyses confirm the significant impact of the cutting sequence on the chip removal process of CFRP/Ti6Al4V stacks.

Additionally, the surface morphologies resulting from cutting are the evidence characterizing the material removal process of the workpieces. Figs. 8 and 9 show the three-dimensional (3D) topographies of machined CFRP/Ti6Al4V surfaces over a scanning area of 0.9 mm × 1.2 mm gained under different cutting sequences. It can be seen that the CFRP surfaces generated in the Ti → CFRP sequence appear relatively rougher than those produced in the CFRP → Ti sequence. This is attributed to the scratching effects of the titanium chip adhesion on the composite surfaces as discussed earlier. The damage modes of the cut CFRP surfaces in the 3D topographic maps are featured by surface cavities/cracking due to the loss of carbon/epoxy materials in cutting. The titanium surfaces generated in the stack machining are basically composed of uniform feed marks and grooves running perpendicular to the tool cutting direction. The deformation of feed marks occurs mainly due to the plastic flow of the metallic phase in the cutting process, which may contribute to higher surface roughness values as well as higher residual stress levels. The interface region linking the metallic phase and the composite phase depicts irregular surface profiles and heights due to the heterogeneity in structures. Regarding the quantitative analysis of the machined stack quality, cutting from the CFRP to Ti is confirmed benefiting the improvement of the stack surface finish. Detailed results can be referenced in our previous studies [11,12], which are thereby not discussed here.

3.2. Stack interface machining

Machining the two stacked constituents simultaneously involves a coupling chip separation mode of brittle fracture and elastoplastic deformation, which signifies the characteristics of the interface drilling. Fig. 10 depicts the force signals (F_c and F_t) recorded in the 0 °CFRP/Ti6Al4V interface machining under the cutting conditions of v_c = 50 m/min and a_p = 0.20 mm. It is apparent that the force signatures measured in the stack interface machining appear very scattered. This should not be considered as noise, but as the consequences of the varying fiber cutting modes as well as the serrated chip formation of the titanium alloy. Contrary to the orthogonal cutting under different cutting sequences, the stack interface machining basically involves three stages. The first stage I denotes a gradual engagement of the tool-work interaction, in which both the cutting and thrust forces undergo a rapid increasing trend. When the tool edge fully participates in the bi-material machining, the cutting process seems to reach a steady status as exhibited in stage II of Fig. 10, where both F_c and F_t magnitudes

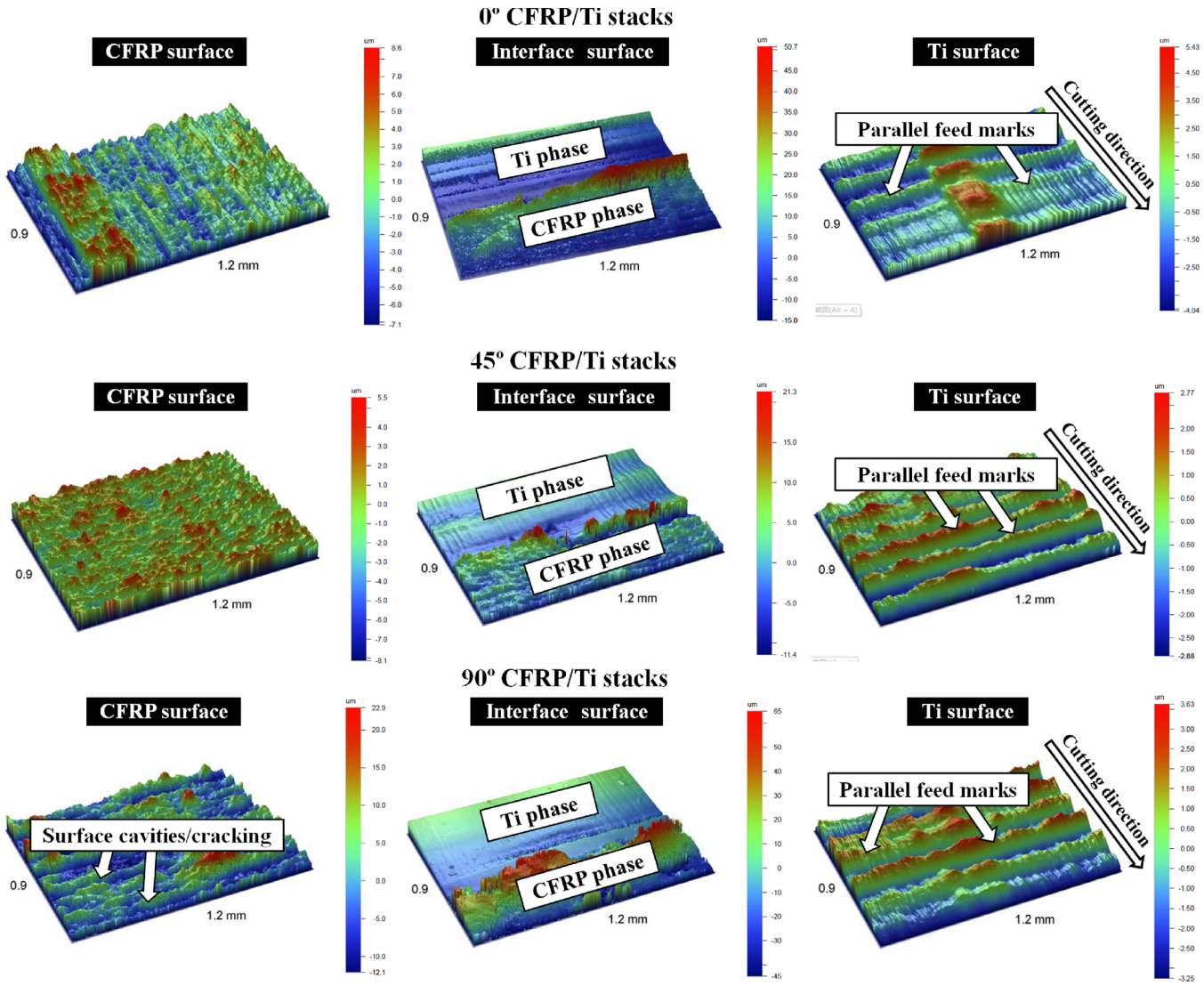

Fig. 9. 3D topographies of the machined stack surfaces under the Ti → CFRP sequence (v_c = 50 m/min and a_p = 0.20 mm).

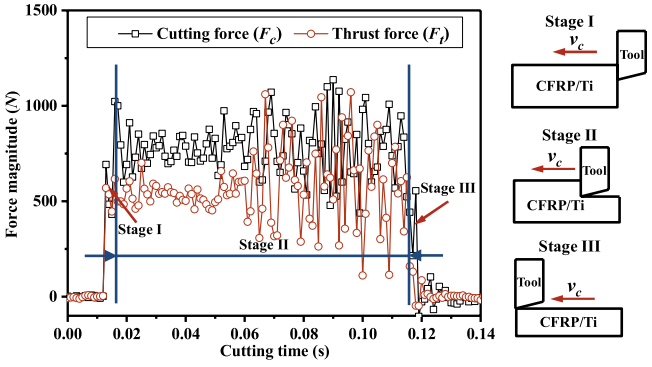

Fig. 10. Evolution of the force profiles during the stack interface machining (v_c = 50 m/min and a_p = 0.20 mm).

experience a cyclic variation process. As the tool edge tends to exit the multilayer stack, the F_c and F_t signals decrease quickly into zero, which signifies the final cutting stage III.

High-speed CCD camera images of the *in-situ* material removal process during the CFRP/Ti6Al4V interface cutting are shown in Fig. 11. The entire chip separation process of the stack can be considered as a summation of individual composite cutting and titanium alloy machining since no interrelated machining phenomena between the two stacked phases occur in the present cutting configuration. When the tool edge cuts into the two stacked materials simultaneously, serrated and powdery chips are both produced on the tool rake face. In machining either a 0° UD-CFRP or a 90° UD-CFRP laminate, the resected chips are basically in the form of tiny fragments as evidenced in Fig. 11 due to the predominance of the brittle-fracture mechanism. In the case of machining a 0° CFRP, the composite chips are generally produced accompanied by the peel fracture, interfacial debonding and fiber fracture while for the 90°CFRP laminate, the tool edge starts cutting perpendicular to the fiber axis and tends to shear and bend the chips being cut, leading to serious fiber/matrix splintering occurring far beyond the machined surface (Ref. Fig. 11(b)) due to the out-of-plane fracture propagating along the fiber/matrix interface with severe macro deformation induced by the compressive tool load. In cutting the stacked titanium alloy, serrated chip formation is noted throughout the entire cutting process. This is attributed to the elastoplastic deformation mode dominating the material removal process. Moreover, since both materials show disparate chip separation modes, the tool edge engaged in the bi-material machining should suffer uneven distributions of stresses and temperatures, which may cause severe tool-work instability possibly increasing the risk of catastrophic tool failures like micro-chipping or edge fracture.

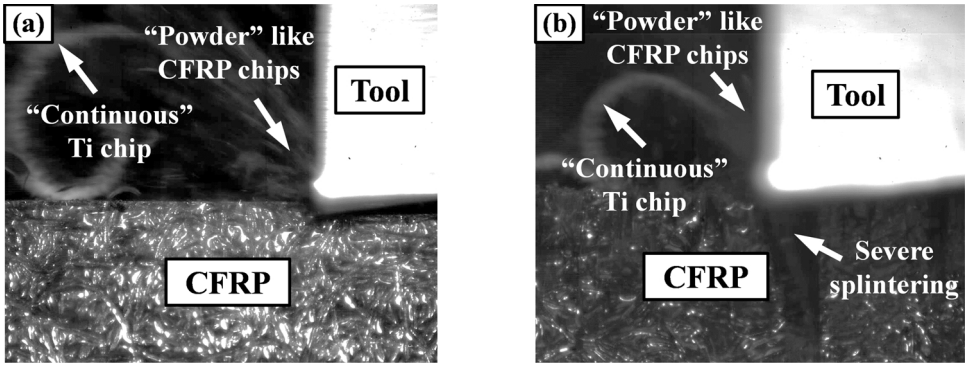

Fig. 11. *In-situ* chip separation process of CFRP/Ti6Al4V interface machining (v_c = 50 m/min and a_p = 0.20 mm): (a) $\theta = 0^\circ$ and (b) $\theta = 90^\circ$.

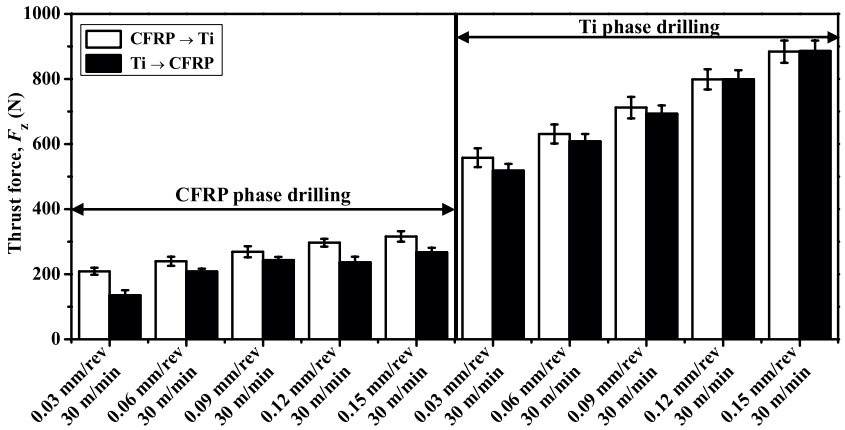

Fig. 12. Comparative thrust force magnitudes between two different cutting sequence strategies in drilling of CFRP/Ti6Al4V stacks at various feed rates (Ref. [16]).

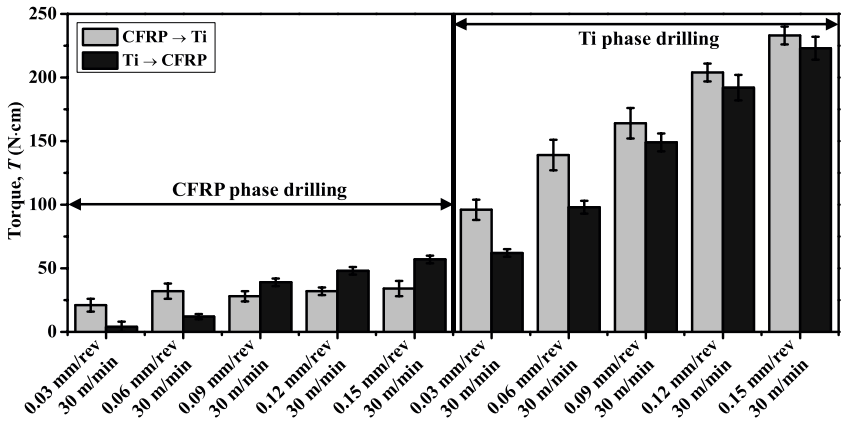

Fig. 13. Comparative torque magnitudes between two different cutting sequence strategies in drilling of CFRP/Ti6Al4V stacks at various feed rates (Ref. [16]).

3.3. Drilling of CFRP/Ti6Al4V stacks

3.3.1. Drilling forces

Drilling force signals which are determined by the interacting behavior of the tool-workpiece-parameter system play a vital role in characterization of the *in-situ* tool-work interaction associated with the chip removal mode. Owing to the dissimilar machinability of CFRP composites and titanium alloys, the force signals developed in the bi-material drilling as a function of cutting time can be classified into five stages that entail the initial/full engagements of the composite drilling, the interface drilling and the initial/full engagements of titanium drilling. The engagements of either CFRP drilling or Ti drilling can be considered as the individual machining operations of composites and metal alloys while the interface drilling remains analogous to the combined interface machining in which both the two stacked constituents are being cut simultaneously. A detailed analysis of the drilling force signatures for CFRP/Ti6Al4V stacks was provided in our previous experimental work [16]. Thus the present subsection concerns only the parametric effects on the magnitudes of the drilling forces produced in the stack drilling. Figs. 12 and 13 show the results of the thrust force (F_z) and torque (T) in terms of different drilling sequences. It is noted that the feed rate has a great impact on the drilling thrust and torque of both the CFRP and Ti phases. High thrust forces and torques are produced under the conditions of high feed rates, which increases the risk of delamination and burr formation being detrimental to the quality of drilled holes. In both cutting sequences, drilling the titanium phase commonly produces much higher magnitudes of the thrust force and toque than the CFRP phase drilling. The findings agree well with the

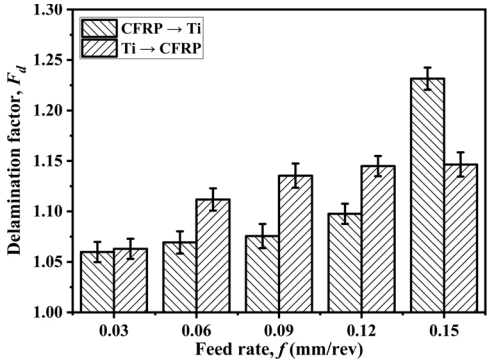

Fig. 14. Comparative results of the delamination factors (F_d) gained under different drilling sequences.

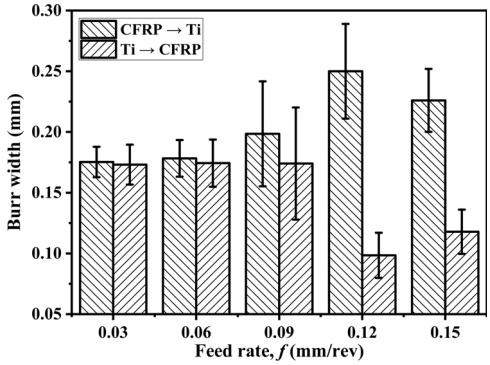

Fig. 15. Comparative results of the burr width gained under different drilling sequences.

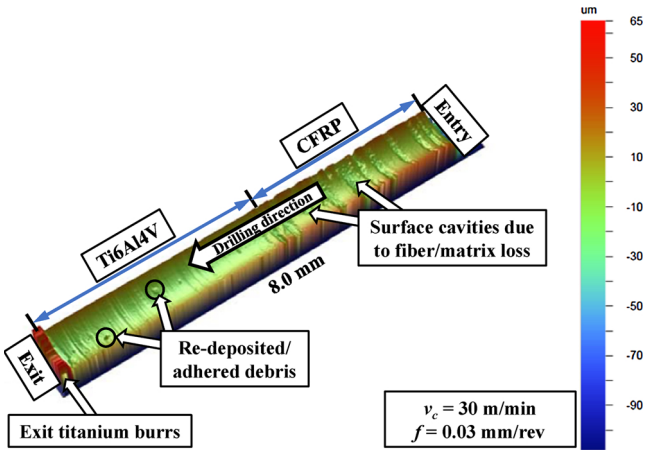

Fig. 16. 3D topographies of a stack hole drilled under the CFRP → Ti sequence.

observation in the aforementioned stack orthogonal cutting. Moreover, it is worth noting that the CFRP → Ti drilling promotes relatively higher force magnitudes for both the CFRP phase and the Ti phase as shown in Figs. 12 and 13. The phenomenon is mainly due to the scratching effect of the titanium chip evacuation on the cut composite surfaces under the CFRP → Ti drilling sequence which influences the force measurement.

3.3.2. Drilling-induced damage

The poor machinability of CFRP/Ti6Al4V stacks is often manifested by the serious mechanically/thermally-induced damage of the cut surfaces. Amongst the defects caused by drilling, delamination occurring in the composite phase and burrs promoted in the metallic phase are critical concerns since they adversely affect the structural integrity of the stack materials. In this work, the most-used one-dimensional delamination factor (F_d) and the burr width indicator were utilized to quantify the damage extents of drilled CFRP/Ti6Al4V holes. The obtained results are depicted in Figs. 14 and 15. It is clear that the delamination factors of the drilled CFRP/Ti6Al4V holes correlate with the utilized drilling parameters. The feed rate shows a significantly positive impact on the delamination extents for both the implemented cutting sequences (Ref. Fig. 14). The maximum delamination extents often result from the use of the highest feed rate (*i.e.* f = 0.15 mm/rev) due to the highest thrust force produced in the stack drilling (Ref. Fig. 12). Additionally, the CFRP → Ti sequence generally produces relatively lower extents of delamination compared with the Ti → CFRP drilling sequence owing to the supporting role of the bottom Ti plate in increasing the stiffness of the exit CFRP layers.

Moreover, the impact of the feed rate on the burr width is observed totally positive or negative, depending on the used cutting sequence as shown in Fig. 15. In most cases, drilling from Ti to CFRP facilitates the decrease of the burr width compared with the CFRP → Ti drilling sequence under the identical cutting conditions. When the CFRP/Ti6Al4V stacks are drilled under the lowest feed rate conditions (*i.e.* f = 0.03 mm/rev), both two cutting sequences produce approximately the comparable magnitudes of the burr width around 0.175 mm. Increasing the feed rate tends to decrease the burr severity for the Ti → CFRP sequence due to the reduced cutting temperatures with the elevated feed rate and the backup of the CFRP plate. However, a contrary trend between the burr width and the feed rate is identified for the drilling strategy from CFRP to Ti. From the aspect of minimizing the burr formation, the Ti → CFRP cutting sequence should be adopted in drilling CFRP/Ti6Al4V stacks as it can produce lower burr widths particularly when high feed rates are used (Ref. Fig. 15).

3.3.3. Topographies of drilled holes

Fig. 16 shows an overall 3D topographies of a hole drilled under the CFRP → Ti sequence (v_c = 30 m/min and f = 0.03 mm/rev). Observations indicate that the surface morphologies of the Ti hole appear much smoother than those of the drilled composite and interface. Serious surface cavities/cracking due to the loss of fiber/matrix materials are clearly visible particularly at the 135° orientated plies of the machined CFRP hole. During machining, fibers in the 135° direction are typically subjected to intense elastic bending combined with out-of-plane shear fracture induced by the compressive tool load [15,17]. As the local stress exceeds the strength limit of fibers, failure occurs below the cutting plane with the debris removed as the tool passes, which creates cavities on the surface [17]. On the other hand, since the titanium alloy is drilled after the CFRP phase, the ejection of the hot and shape-edged titanium chips should cause severe abrasions/scratches onto the composite surfaces, thus exacerbating the damage extents. In contrast, the damage modes of the drilled titanium surfaces are featured by re-deposited debris, deformation of feed marks and exit burrs as depicted in Fig. 16.

Additionally, Figs. 17–21 show the topographies of the inner CFRP/Ti6Al4V holes produced under the varying feed rate. The results confirm the similar damage modes of a drilled stack hole observed in Fig. 16. Besides, the feed rate is found to have a great impact on the stack hole quality such that increasing the feed rate tends to significantly deteriorate the surface finish of the CFRP/Ti6Al4V holes. This is evidenced by the increased severity of surface cavities/cracking in the composite phase and the intensified feed marks/grooves of drilled titanium surfaces with the elevated feed rate. The phenomenon is mainly due to the increased drilling forces as the feed rate increases. The titanium phase is identified capable of maintaining higher hole quality compared with the CFRP one due to its inherent homogeneity in properties. Surface cavities and cracking are the characteristic damage of drilled CFRP surfaces while feed marks, adhered debris are features of the titanium surface imperfections. The observations are consistent with the findings in the orthogonal cutting of CFRP/Ti6Al4V stacks.

To identify the impact of the drilling sequence on the stack hole

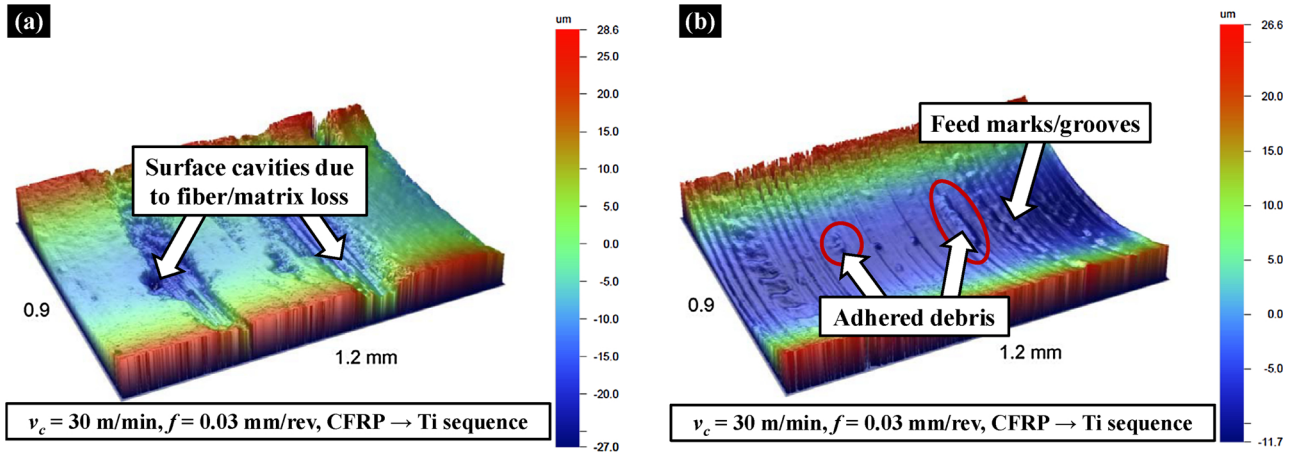

Fig. 17. 3D topographies of a stack hole: (a) CFRP hole and (b) Ti hole (v_c = 30 m/min and f = 0.03 mm/rev).

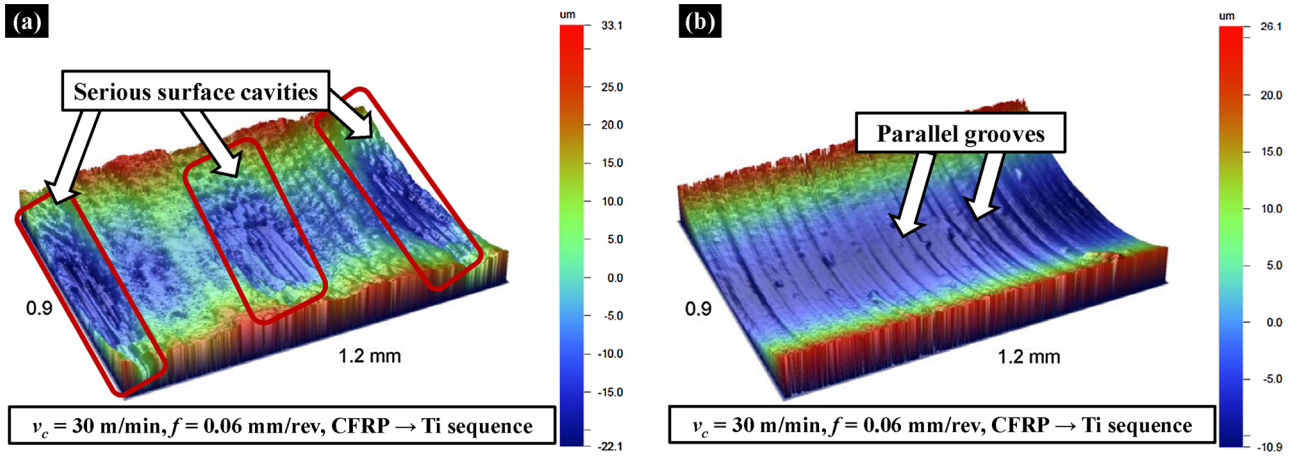

Fig. 18. 3D topographies of a stack hole: (a) CFRP hole and (b) Ti hole (v_c = 30 m/min and f = 0.06 mm/rev).

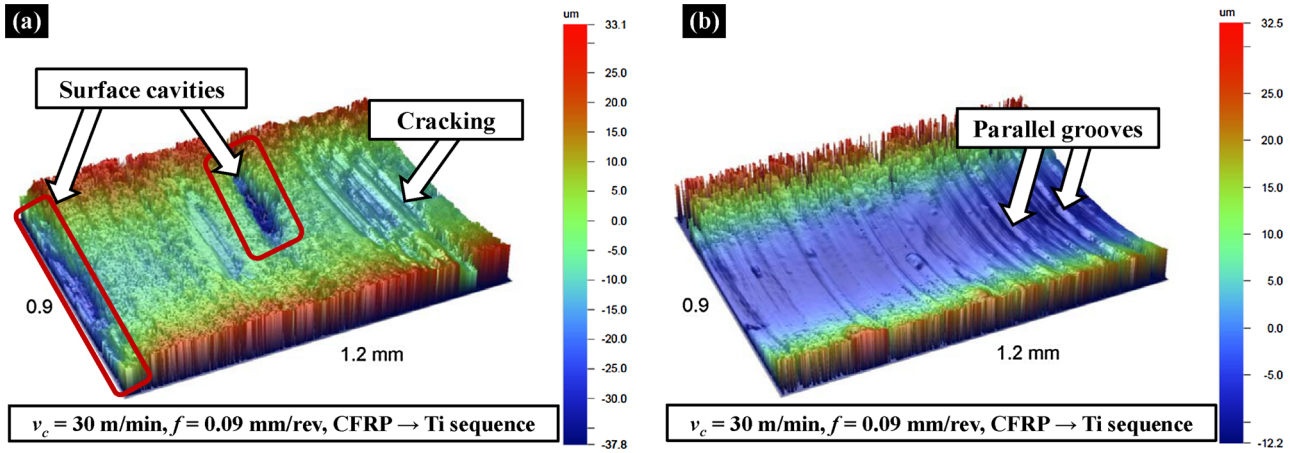

Fig. 19. 3D topographies of a stack hole: (a) CFRP hole and (b) Ti hole (v_c = 30 m/min and f = 0.09 mm/rev).

surfaces, the 3D topographies and SEM morphologies of CFRP/Ti6Al4V holes drilled under the constant conditions of v_c = 30 m/min and f = 0.03 mm/rev are shown in Figs. 22–24. It is clear that the cutting sequence strategy has an obvious effect on the CFRP/Ti6Al4V surfaces. Drilling the multilayer stacks in the CFRP → Ti sequence tends to result in more serious fiber/matrix cracking of the composite surfaces than the opposite drilling sequence. This is attributed to the severe scratching effects of the sharp-edged titanium chips onto the polymeric hole wall surfaces that severely deteriorate the composite surface integrity during the ejection process. Additionally, the Ti hole surfaces drilled in both cutting sequences appear much smoother than those of the CFRP phase and interface due to the chip separation mode of elastoplastic deformation. The findings are consistent with the observations during the stack orthogonal cutting. The major damage modes of the cut CFRP hole surfaces are found depending on the utilized drilling sequence. When drilling from CFRP to Ti interlaminar cracking due to the detrimental effects of the titanium chip evacuation operates as a key damage mode for the CFRP hole surfaces while matrix

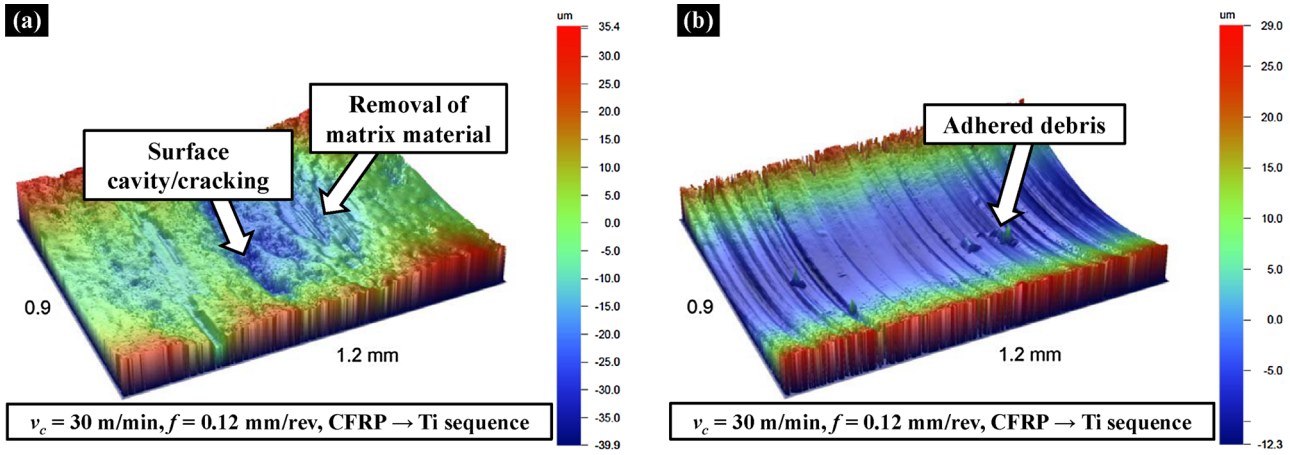

Fig. 20. 3D topographies of a stack hole: (a) CFRP hole and (b) Ti hole (v_c = 30 m/min and f = 0.12 mm/rev).

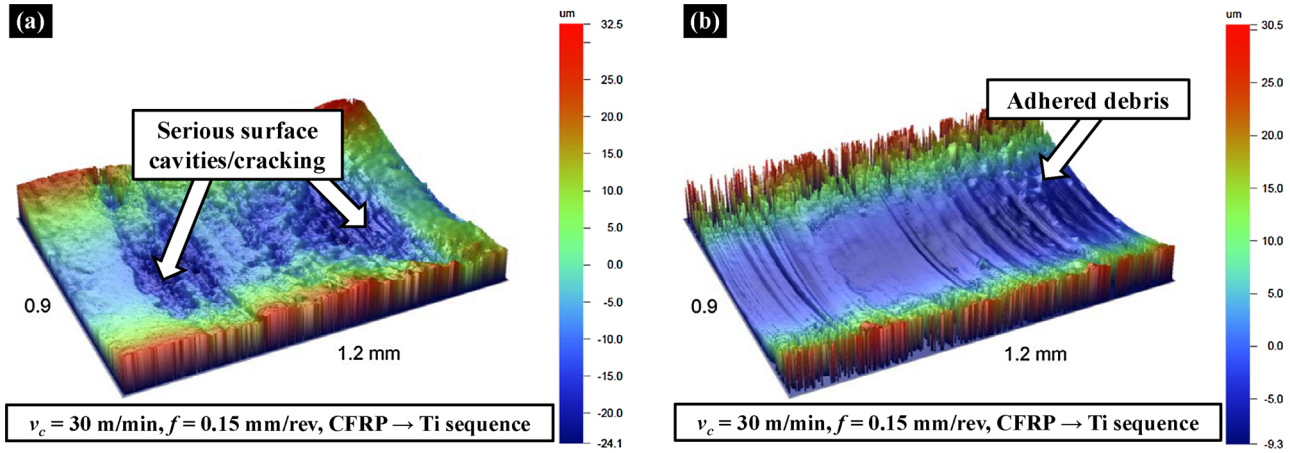

Fig. 21. 3D topographies of a stack hole: (a) CFRP hole and (b) Ti hole (v_c = 30 m/min and f = 0.15 mm/rev).

	Drilled stack holes		
	CFRP phase	Interface	Ti phase
CFRP → Ti	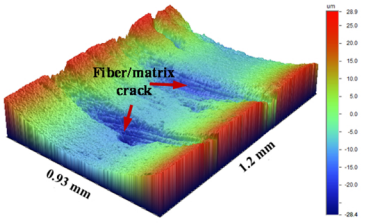	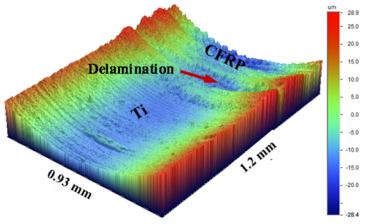	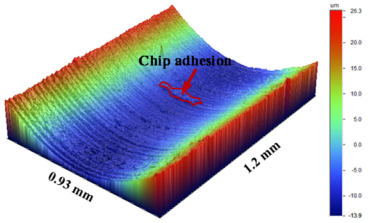
Ti → CFRP	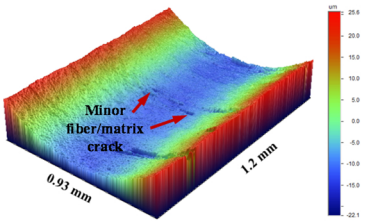	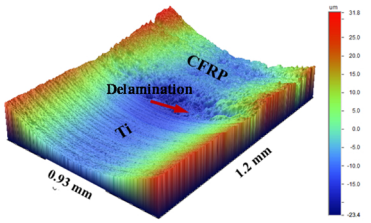	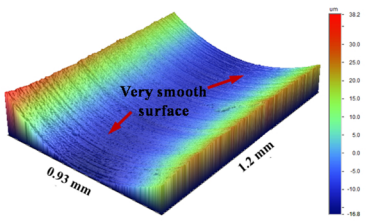

Fig. 22. Comparative hole topographies under different drilling sequences (v_c = 30 m/min and f = 0.03 mm/rev).

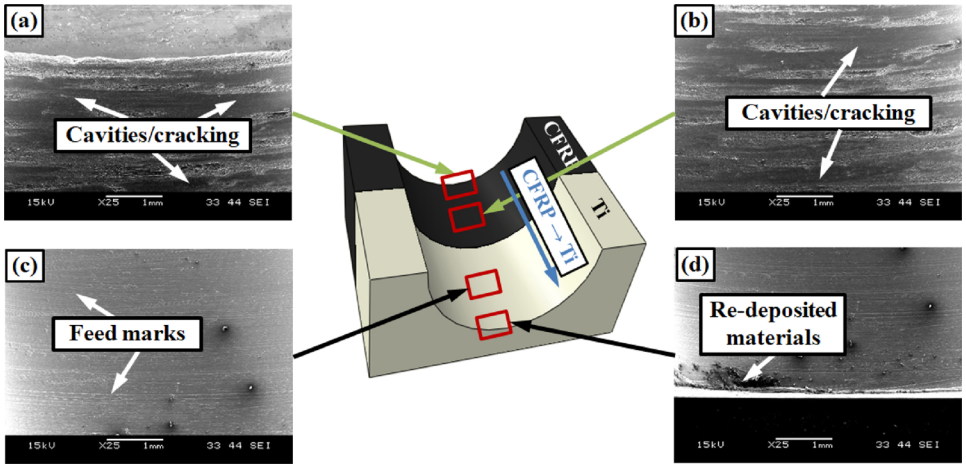

Fig. 23. SEM images of the drilled CFRP/Ti6Al4V hole morphologies under the CFRP → Ti cutting sequence: (a) entry CFRP surface, (b) middle CFRP surface, (c) middle Ti surface, and (d) exit Ti surface.

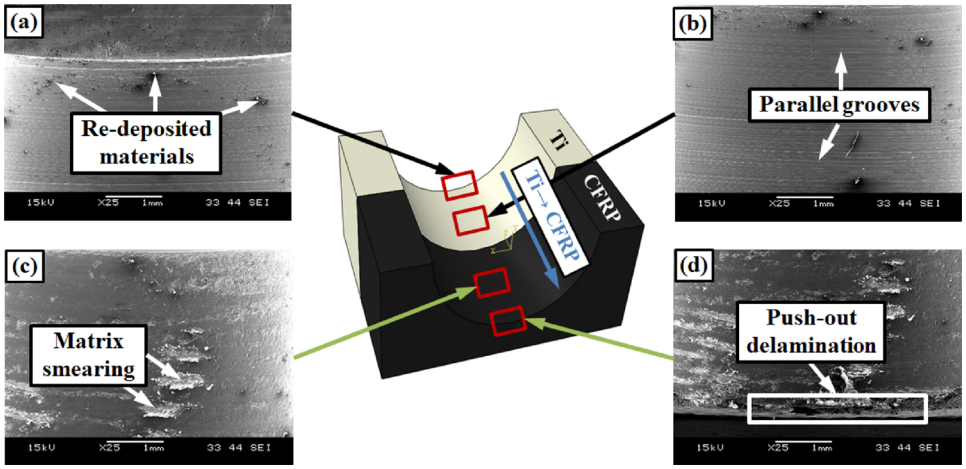

Fig. 24. SEM images of the drilled CFRP/Ti6Al4V hole morphologies under the Ti → CFRP cutting sequence: (a) entry Ti surface, (b) middle Ti surface, (c) middle CFRP surface, and (d) exit CFRP surface.

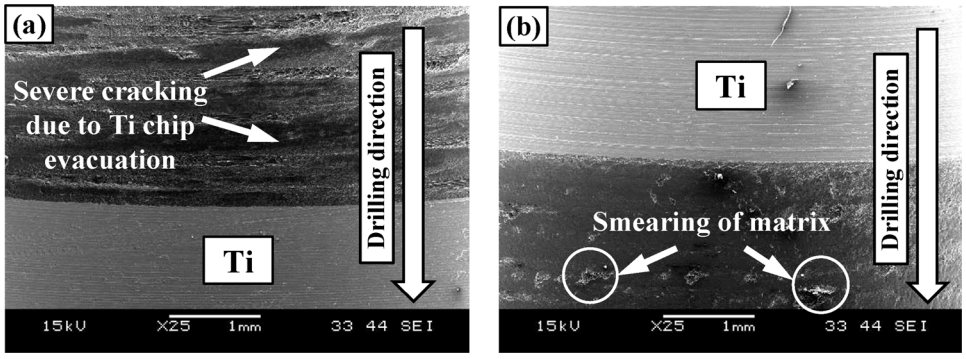

Fig. 25. SEM images of the stack interface morphologies gained under (a) the CFRP → Ti sequence and (b) the Ti → CFRP sequence (v_c = 30 m/min and f = 0.03 mm/rev).

smearing and push-out delamination characterize the damage types of drilled CFRP holes under the Ti → CFRP drilling sequence. The main defects occurring in the drilled titanium holes are featured by deformation of feed marks and re-deposited chip materials onto the already machined surfaces. The deformation of feed marks occurs mainly due to the plastic flow of the metallic phase in the cutting process [18], which may contribute to higher surface roughness values as well as higher residual stress levels. The deposited materials onto the titanium surface may originate from the resected chips under the conditions of high cutting pressures and temperatures during the stack drilling, which are detrimental to the functionality of the machined components.

In the multilayer stack drilling, the interface represents the most difficult-to-cut zone susceptible to serious damage as discussed earlier in subsection 3.1. Fig. 25 details the comparative SEM images of the drilled stack interface morphologies under two different drilling sequences. The SEM inspections reveal that the interface damage occurs mainly close to the machined CFRP phase. The CFRP → Ti drilling induces severe composite surface damage approaching the interface zone

due to the scratching effects of the titanium chip evacuation on the drilled CFRP phase. By contrast, the interface damage promoted in the Ti → CFRP drilling sequence is limited owing to the avoided effects of the metallic chip ejection. The above analysis indicates the potential benefits of utilizing the Ti → CFRP drilling sequence in improvement of the stack hole quality. The findings contradict the conclusions drawn in the orthogonal cutting of the CFRP/Ti6Al4V stacks as the titanium chip ejection indeed has an impact on the drilled composite surfaces while drilling.

4. Conclusions

The present work concerns an experimental study of the machinability of aerospace grade CFRP/Ti6Al4V stacks. Both the orthogonal cutting and the stack interface machining were designed to facilitate the stack drilling. Based on the results acquired, the following key conclusions can be drawn.

- The orthogonal cutting analysis reveals a combined chip separation mode of brittle fracture and elastoplastic deformation dominating the stack cutting process, which results in discontinuous and serrated chip formation. The machinability of CFRP/Ti6Al4V stacks is found to be fiber orientation dependent such that increasing the fiber orientation leads to difficult composite chip separation and hence severe subsurface damage of the stack.
- The cutting sequence strategy has a significant effect on both the orthogonal cutting and the hole drilling of CFRP/Ti6Al4V stacks, which is manifested by the impacts of the metallic chip adhesion on the post CFRP cutting for the orthogonal cutting and by the scratching effects of the titanium chip ejection on the cut composite surfaces.
- Both the feed rate and drilling sequence have a great impact on drilling forces, delamination extents and titanium burrs. Defects of the drilled stack interface exist mainly in the adjacent composite phase. The cut composite hole defects are featured by the interlaminar cracking, matrix smearing and delamination, while the titanium hole defects are mainly the deformation of feed marks and re-deposited chip materials.
- Moreover, the most-used CFRP → Ti sequence is not totally reasonable for the one-shot drilling of CFRP/Ti6Al4V stacks. In contrast, drilling from Ti to CFRP in some sense would be a more preferred strategy as it provides more drilling advantages over the counterpart one such as lower drilling forces, lower burr extents, better hole surface morphologies.

Acknowledgments

The authors gratefully acknowledge the financial support of the National Natural Science Foundation of China (Grant No.51705319), Shanghai Pujiang Program (Grant No.17PJ1403800) and Shanghai Academy of Spaceflight Technology (Grant No. SAST2017-060). The work is also partly sponsored by the Research Project of State Key Laboratory of Mechanical System and Vibration (Grant No. MSVZD201704).

References

[1] Brinksmeier E, Fangmann S, Rentsch R. Drilling of composites and resulting surface integrity. CIRP Ann Manuf Technol 2011;60(1):57–60.
[2] Xu J, Mkaddem A, El Mansori M. Recent advances in drilling hybrid FRP/Ti composite: a state-of-the-art review. Compos Struct 2016;135:316–38.
[3] Impero F, Dix M, Squillace A, Prisco U, Palumbo B, Tagliaferri F. A comparison between wet and cryogenic drilling of CFRP/Ti stacks. Mater Manuf Process 2018;33(12):1354–60.
[4] Kim D, Beal A, Kwon P. Effect of tool wear on hole quality in drilling of carbon fiber reinforced plastic–titanium alloy stacks using tungsten carbide and polycrystalline diamond tools. J Manuf Sci Eng-Trans ASME 2016;138(3):031006.
[5] Ramulu M, Branson T, Kim D. A study on the drilling of composite and titanium stacks. Compos Struct 2001;54(1):67–77.
[6] Isbilir O, Ghassemieh E. Comparative study of tool life and hole quality in drilling of CFRP/titanium stack using coated carbide drill. Mach Sci Technol 2013;17(3):380–409.
[7] Park KH, Beal A, Kim D, Kwon P, Lantrip J. Tool wear in drilling of composite/titanium stacks using carbide and polycrystalline diamond tools. Wear 2011;271(11-12):2826–35.
[8] Prabukarthi A, Senthilkumar M, Krishnaraj V. Study on drilling of CFRP/Ti6Al4V stack with modified twist drills using acoustic emission technique. Steel Compos Struct 2016;21(3):573–88.
[9] Cong W, Pei Z, Treadwell C. Preliminary study on rotary ultrasonic machining of CFRP/Ti stacks. Ultrasonics 2014;54(6):1594–602.
[10] Sanda A, Arriola I, Navas VG, Bengoetxea I, Gonzalo O. Ultrasonically assisted drilling of carbon fibre reinforced plastics and Ti6Al4V. J Manuf Process 2016;22:169–76.
[11] Xu J, El Mansori M. Experimental studies on the cutting characteristics of hybrid CFRP/Ti stacks. Procedia Manuf 2016;5:270–81.
[12] Xu J, El Mansori M. Wear characteristics of polycrystalline diamond tools in orthogonal cutting of CFRP/Ti stacks. Wear 2017;376-377:91–106.
[13] Grzesik W, Zalisz Z, Król S. Tribological behaviour of TiAlN coated carbides in dry sliding tests. J Achiev Mater Manuf Eng 2006;17(1-2):181–4.
[14] Meena A, El Mansori M. Study of dry and minimum quantity lubrication drilling of novel austempered ductile iron (ADI) for automotive applications. Wear 2011;271(9):2412–6.
[15] Wang DH, Ramulu M, Arola D. Orthogonal cutting mechanisms of graphite/epoxy composite. Part I: unidirectional laminate. Int J Mach Tools Manuf 1995;35(12):1623–38.
[16] Xu J, El Mansori M. Experimental study on drilling mechanisms and strategies of hybrid CFRP/Ti stacks. Compos Struct 2016;157:461–82.
[17] Li MJ, Soo SL, Aspinwall DK, Pearson D, Leahy W. Influence of lay-up configuration and feed rate on surface integrity when drilling carbon fibre reinforced plastic (CFRP) composites. Procedia CIRP 2014;13:399–404.
[18] Ezugwu EO, Bonney J, Da Silva RB, Çakir O. Surface integrity of finished turned Ti-6Al-4V alloy with PCD tools using conventional and high pressure coolant supplies. Int J Mach Tools Manuf 2007;47(6):884–91.